Ecological Indicators 150 (2023) 110250

Contents lists available at ScienceDirect

Ecological Indicators

journal homepage: www.elsevier.com/locate/ecolind

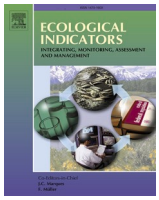

Original Articles

Can economic growth and urban greenness achieve positive synergies during rapid urbanization in China?

Min Cheng [a,b], Shaohua Wu [a,*], Canying Zeng [a], Xiaolu Yu [a], Jingyi Wang [a]

[a] Institute of Land and Urban-Rural Development, Zhejiang University of Finance and Economics, Hangzhou 310018, China
[b] Institute of "Eight-Eight" Strategies of Zhejiang, Hangzhou 310018, China

ARTICLE INFO

Keywords:
Urbanization
Incoordination
Economic growth
Urban greenness
Nighttime light

ABSTRACT

Rapid urban expansion reflects the increasing economic growth in China. As an original conceive for urban sustainability, economic growth contributes to vegetation changes. However, the spatiotemporal heterogeneity of the relationships between these two factors remains unclear in China. After analyzing the spatiotemporal characteristics of the urban expansion in different cities in China from 2002 to 2020, we found a rapid and continuous urban expansion in China, with the mean annual expansion of 1710.96 km^2 $year^{-1}$ ($p < 0.01$). However, based on the trends of annual maximum enhanced vegetation index (EVI_{max}) and the nighttime light (NTL), a strong incoordination status (areas with significant increasing NTL ($p < 0.05$) but significantly decreasing EVI_{max}) between urban greenness and economic growthwas found during this rapid urban expansion period. Spatially, >60% of cities showed incoordination status and 38.08% of cities showed strongly incoordination status. At pixels levels, these strong incoordination status in urban areas can be fully explained by long-term average NTL digital Number (DN) gradient.Based on a piecewise linear regression model, the proportion of areas with the strong incoordination status was significantly increased by the 1.07% DN^{-1} ($p < 0.01$) when multi-year average NTL value is <50, but decreased strongly afterward, with the slope of −2.96% DN^{-1} ($p < 0.01$). The strong incoordination between urban greenness and economy can be rapidly mitigated with the rapid economic growth. This threshold can be a critical indicator for decision-makers in identifying and analyzing the status of ecological civilization in various regions of China.

1. Introduction

Urbanization involves a set of economic and environmental processes, which was regarded as a key to deeply influence the regional sustainable development (Wu et al., 2011; Normile, 2016; Ning et al., 2022). This process also gets facilitated by the horizontal expansion of cities, that is, the increase in urban built-up areas. According to a recent study, the 68% of the global population will live in urban areas by 2050 (Sun et al., 2020). In addition, China's urbanization rate has increased from 17.92% to 52.57 % in recent decades (Liu et al., 2016). Undoubtedly, this population growth and migration from rural to urban areas will produce a concomitant increased demand for urban built-up areas and a development of regional economies. However, this rapid process of urbanization showed spatial heterogeneity across the different regions and cities in China because of its different social and economic development and the different land policy (Wu et al., 2011; Chen et al., 2016; Jia et al., 2020; Feng and Wang, 2022). During this rapid urbanization, it is important to obtain the accurate spatial information of economy to explore the different relationships of urban greenness and economic growth. However, traditional statistics cannot be used to identify the spatial characteristics of economic growth in different urban areas. In contrast, it has been found that nighttime light data (NTL) provides a unique perspective on the artificial light intensity at the pixels scale, which is widely used for monitoring the spatially explicit dynamics of economic growth (Shi et al., 2014; Zhou et al., 2018; Levin et al., 2020; McCallum et al., 2022; Zhao et al., 2022). For instance, Shi et al. (2014) investigated the potential of NTL data in modeling gross domestic product (GDP) at multiple scales and found that NTL are effective for modeling socioeconomic changes. Recently, based on calibrated NTL, Chen et al. (2022a) obtained a continuous global gridded GDP dataset during 1992–2019. Therefore, in order to analyze economic growth in each urban pixel, this NTL were used in our study.

The complexities of the economy-environment dynamic compromise

* Corresponding author.
E-mail address: shaohua@zufe.edu.cn (S. Wu).

https://doi.org/10.1016/j.ecolind.2023.110250
Received 30 November 2022; Received in revised form 2 April 2023; Accepted 11 April 2023
Available online 17 April 2023

the goal of achieving urban sustainable development (Dobbs et al., 2017; Fu et al., 2019; Fu et al., 2020; He et al., 2020). Sustainable urban development depends on economic growth, while such growth also influences essential ecosystem functions in urban areas. On the one hand, the vegetation degradation caused by rapid urbanization and economic growth was demonstrated in many previous studies, (Zhao et al., 2013; Dobbs et al., 2017; Liu et al., 2019; Yang et al., 2022a), which further exacerbates the challenges and risks of the urban ecological environment (He et al., 2020; Yang et al., 2022a). On the other hand, with this rapid economic growth, many resources have been invested in the construction of infrastructure to improve the urban ecological environment (Lu et al., 2019; Jia et al., 2020). Therefore, vegetation greening was also observed in many urban areas (Ruan et al., 2019; Li et al., 2020a; Sun et al., 2020; Cui et al., 2022; Wang et al., 2022). For example, Li et al. (2020a) found that about 63 % of the areas in urban environments in China showed greening trends during 2000–2013. Similarly, based on the satellite-derived enhanced vegetation index in 1500-plus cities in China during 2000–2019, Li et al. (2023) found this significant greening in urban core areas.

Generally, a significant spatial differentiation of the relationship between urban greenness and economic growth was observed in the urban cores and fringes. In other word, despite the rapid economic growth, the greening trends gradually decreased from urban cores to newly urbanized areas. Previous studies have already demonstrated the vegetation degradation in many study areas (Lin and Wu, 2019; Liu et al., 2020), and explored the spatial variations in vegetation greening in urban areas (Sun et al., 2020; Shahtahmassebi et al., 2021; Cui et al., 2022; Yang et al., 2022b). However, due to the different socioeconomic levels of different sub-regions, the spatiotemporal heterogeneity of the relationship between urban greenness and economic growth is uneven in China. Hence, it is of value to consider spatial heterogeneity in different regions of China. Furthermore, this spatial differentiation pattern implies the possibile threshold effect, which represents the economy boundary conditions for achieving positive synergy between urban economic growth and greenness. But this possible threshold is rarely quantified in previous studies. Therefore, the main focus of this research was on the following questions: (1) During the rapid urbanization period, which relationships exist between economic growth and vegetation dynamics in different cities and regions? (2) whether economic growth and urban greenness can achieve positive synergies during this period. (3) Providing scientific thresholds for urban economy that can promote a synergistic relationship between urban greenness and economic growth. This quantitative and better study of this scientific threshold will be a critical indicator for decision-makers in identifying and analyzing the status of ecological civilization in different regions of China.

2. Materials and methods

2.1. Study area

In this study, we explored the spatiotemporal variations of urban expansion and the relationship between urban greenness and economic growth in 344 cities in China. Specifically, in the context of coordinated regional development policy in China, two different administrative levels were selected for multi-scale analysis (Fig. 1). Firstly, to adequately understand the spatiotemporal heterogeneity of these different relationships, China was divided into Eastern, Central, Western, and Northeastern regions by national bureau of statistics (Available online: https://www.stats.gov.cn/tjzs/cjwtjd/201308/t20130829_74318.html). The socioeconomic development and the process of urbanization of these economic regions were significantly different (Liu et al., 2016; Shi et al., 2016a; Ning et al., 2022), which would affect the different relationships between urban greenness and economic growth. In addition, in order to analyze the spatiotemporal heterogeneity in different urban areas, a further analysis of the different relationships in four typical urban agglomerations was conducted.

2.2. Extraction of urban areas

The urban areas were extracted from the IGBP classification types dataset at 500 m spatial resolution and annual time step during the period of 2001–2020, which was provided by the Moderate Resolution Imaging Spectroradiometer (MODIS) land cover product (MCD12Q1) (Friedl and Sulla-Menashe, 2019). This land cover product has an overall accuracy of 73.6% (Sulla-Menashe et al., 2019) and relatively high

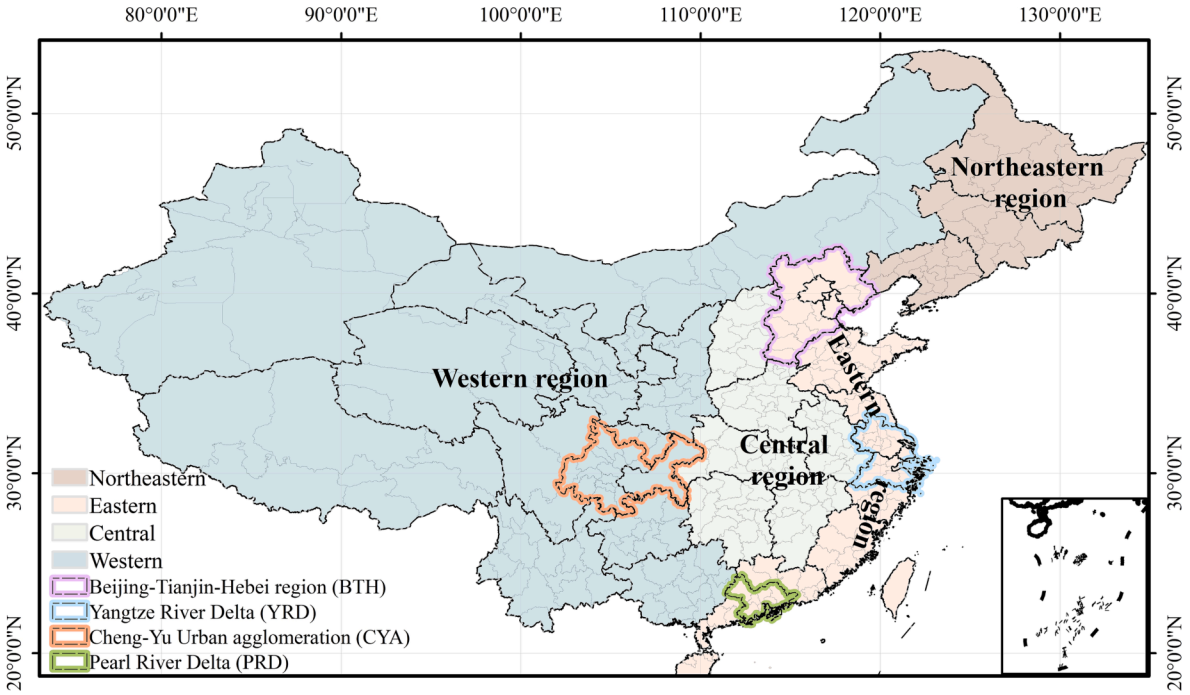

Fig. 1. The spatial distribution of four regions and four urban agglomerations in China.

accuracy for urban areas (Sun et al., 2020). In addition, to identify the spatial heterogeneity of the interannual variability of the economic status and urban greenness and their relationship in different urban areas in each city, urban areas were divided into two parts: central urban areas and newly urbanized areas. The central urban areas refer to the areas which converted to urban and built-up lands before 2002. The newly urbanized areas in each year refer to the pixels changed to urban and built-up area from 2002 to that year.

2.3. The nighttime lights

Previous studies have found that the nighttime light (NTL) provides an insight into the artificial lights intensity which is widely used to explore the spatial characteristics of economic growth in urban areas (Chen and Nordhaus, 2011; Shi et al., 2014; Levin et al., 2020; Chen et al., 2022a). In this study, a harmonized nighttime light dataset was used as the economic growth indicator (downloaded from URL of https://doi.org/10.6084/m9.figshare.9828827 on June-4–2021). The spatial resolution of this harmonized NTL data was 30 arc-seconds. It shows a temporal consistent trend and was tagged in GEOTIFF file format with the digital numbers (DN) ranging from 0 to 63 (Li et al., 2020b). In addition, due to the higher uncertainties in low-DN areas, we only focus on the urban areas with DN values>10 in accordance with the usage notes of this harmonized nighttime light dataset (Li et al., 2020b). Moreover, this harmonized NTL time series data was resampled to 500 m using ArcGIS software to match the spatial resolution of the urban areas. Eventually, the average NTL in the different urban areas was calculated according to the following equation. Meanwhile, a Mann–Kendall test was used to detect the trend of this mean NTL in each city and each urban pixel from 2002 to 2020.

$$NTL_{mean} = \frac{1}{n}\sum_{i=1}^{n} NTL_i \tag{1}$$

where n is the number of urban pixels in each year.NTL_{mean} is the mean NTL of the urban areas. NTL_i indicate the NTL DN values in each pixel.

2.4. Urban greenness data

In our study, the enhanced vegetation index (EVI) at 500 m spatial resolution from 2002 to 2020was used as an indicator of urban greenness, obtained from the MOD13A1 version 6.1 product (Didan, 2021). EVI has greater sensitivity and partially eliminates the effect of canopy background, which is widely used as an effective indicator of urban vegetation status in many studies (Wang et al., 2019; Sun et al., 2020; Wang et al., 2022; Zeng et al., 2022). Moreover, we conducted a Savitzky–Golay filter for this EVI time series to reduce the spurious changes caused by atmospheric contamination and clouds(Cheng et al., 2022). From this EVI time series, the annual maximum EVI (EVI_{max}) was generated to eliminate the influence of vegetation phenology. Similarly, the average EVI_{max} values for each city was calculated. In addition, the trend of the mean EVI_{max} values of each city and the trend of the EVI_{max} for each urban pixel during 2002–2020 were evaluated.

2.5. Defining different relationships between NTL and EVI_{max}

Generally, economic growth has resulted in changes in vegetation dynamics. To evaluate these relationships of urban greenness and economic growth, the decoupling index (DI) was calculated over the period of 2002–2020 according to the following equation (Zhu et al., 2020; Shan et al., 2021).

$$DI = \frac{(EVI^{t1}_{\max} - EVI^{t2}_{\max})/EVI^{t1}_{\max}}{(NTL^{t1} - NTL^{t2})/NTL^{t1}} \tag{2}$$

where $EVI^{t2}_{\max}$, $EVI^{t1}_{\max}$ and NTL^{t2}, NTL^{t1} refers to the mean EVI_{max} values or NTL values in urban areas at the beginning and end of the period, respectively.

Based on this decoupling index, cities were grouped into two categories (DI > 0 and DI < 0). Furthermore, based on the different trends of EVI_{max} and NTL, each category was divided into eight logic possibilities (Table 1).

2.6. The threshold detection

The potential threshold was quantitatively detected using piecewise linear regression (Yuan et al., 2019).

$$y = \begin{cases} \beta_1 x + \beta_0 + \varepsilon \; x \leqslant \alpha \\ \beta_1 x + \beta_2 (x - \alpha) + \beta_0 + \varepsilon \; x > \alpha \end{cases} \tag{3}$$

where x is the multi-year average NTL over 2002–2020; y is the proportion of areas, α is the estimated threshold of average NTL; β_0, β_1, and β_2 are the regression coefficients, and ε is the residual. This piecewise fitting is obtained optimally when the residual sum of squares is minimized (Peng et al., 2017; Hou et al., 2021). All statistical analyses were performed in R version 4.1.2 (R Core Team, 2021). In addition, the Monte Carlo permutation methods (Permutations = 499) were used to test the statistical significance.

3. Results and discussion

3.1. Spatiotemporal characteristics of the urban expansion

Based on the MODIS yearly product, the total urban area in China increased from 140288.68 km^2 to 173762.75 km^2 with the mean annual expansion of 1710.96 km^2 $year^{-1}$ ($p < 0.01$) (Fig. 2a). At regional level, all urban areas in four regions both showed a significant increasing trend ($p < 0.01$) over this period. In particular, the urban expansion rate was

Table 1
Different relationships between EVI_{max} and NTL.

Pattern	Status	DI	Trend of NTL	Trend of EVI_{max}
I	Strong coordination	>0	Significant increasing	Significant increasing
II	Weak coordination	>0	Significant increasing	Nonsignificant increasing
III	Weak coordination	>0	Nonsignificant increasing	Significant increasing
IV	Weak coordination	>0	Nonsignificant increasing	Nonsignificant increasing
V	Strong incoordination	<0	Significant increasing	Significant decreasing
VI	Weak incoordination	<0	Significant increasing	Nonsignificant decreasing
VII	Weak incoordination	<0	Nonsignificant increasing	Significant decreasing
VIII	Weak incoordination	<0	Nonsignificant increasing	Nonsignificant decreasing
IX	Strong negative incoordination	<0	Significant decreasing	Significant increasing
X	Weak negative incoordination	<0	Significant decreasing	Nonsignificant increasing
XI	Weak negative incoordination	<0	Nonsignificant decreasing	Significant increasing
XII	Weak negative incoordination	<0	NonSignificant decreasing	Nonsignificant increasing
XIII	Strong negative coordination	>0	Significant decreasing	Significant decreasing
XIV	Weak negative coordination	>0	Significant decreasing	NonSignificant decreasing
XV	Weak negative coordination	>0	Nonsignificant decreasing	Significant decreasing
XVI	Weak negative coordination	>0	Nonsignificant decreasing	NonSignificant decreasing

DI represents the decoupling index. The significant and nonsignificant trend indicate significance levels of $p < 0.05$ and $p > 0.05$, respectively.

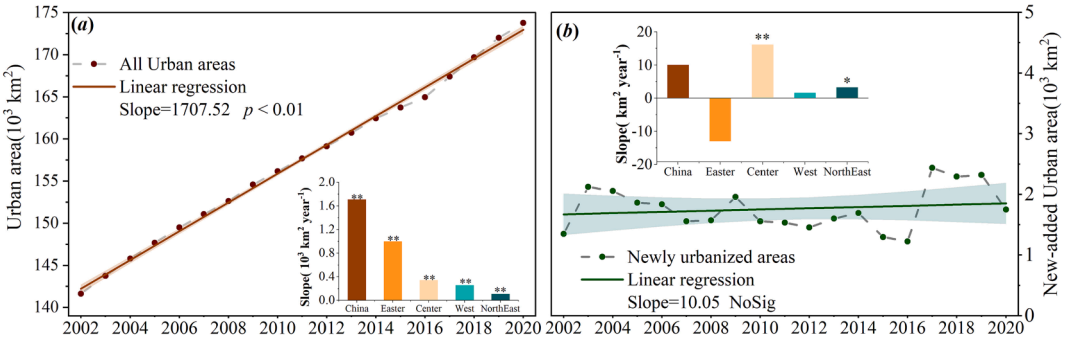

Fig. 2. Interannual variability of the all urban area (a) and annual newly urbanized areas (i.e., pixels that became urban in the current year, b) during the period of 2002–2020. The slope is the average rate of change derived from linear regression derived from linear regression (colored solid line) and the shaded area represents 95% confidence interval. The insets show slopes of all urban areas or annual newly urbanized areas at the regional scale. NoSig indicates the trend is nonsignificant ($p > 0.05$). Symbol ** indicates the trend is significant at levels of $p < 0.01$, and symbol * indicates the trend is significant at levels of $p < 0.05$.

significantly higher in the eastern region than in ohter regions, with the mean annual growth area of 1012.95 km^2 year^{-1}. Almost 59% of the urban expansion took place in the eastern region between 2002 and 2020. While the urban areas in the central, western and northeastern region expanded by an average of 335.14 km^2 year^{-1}, 256.41 km^2 year^{-1}, and 106.46 km^2 year^{-1}, respectively.

Notably, the annual newly urbanized areas (i.e., the pixels changed to urban areas in the current year) in China showed nonsignificant trend ($p > 0.1$), while the interannual variability of annual newly urbanized areas in different regions showed obviously spatial heterogeneity and aggregation effect (Fig. 2b and Fig. 3), with a decreasing trend of −12.91 km^2 year^{-1} in the eastern region and a significantly increasing trend of 16.11 km^2 year^{-1} ($p < 0.01$) in the central region and 3.24 km^2 year^{-1} ($p < 0.05$) in the northeastern region (Fig. 3b). Furthermore, the trends of the annual newly urbanized areas in different aggregations showed obviously spatial heterogeneity (Fig. 3). From 2002 to 2020, the annual newly urbanized areas in BTH showed significant increasing trends (Slope = 10.83 km^2 year^{-1}), yet the significantly decreased trend was found in YRD and PRD, with a decreasing trend of −13.34 km^2 year^{-1} ($p < 0.01$) and −20.66 km^2 year^{-1} ($p < 0.05$). Similarly, the annual newly urbanized areas in CYA showed a decreasing trend during this period.

3.2. Spatiotemporal trend of the nighttime light in urban areas

Urban expansion is driven by urban economic growth. During the

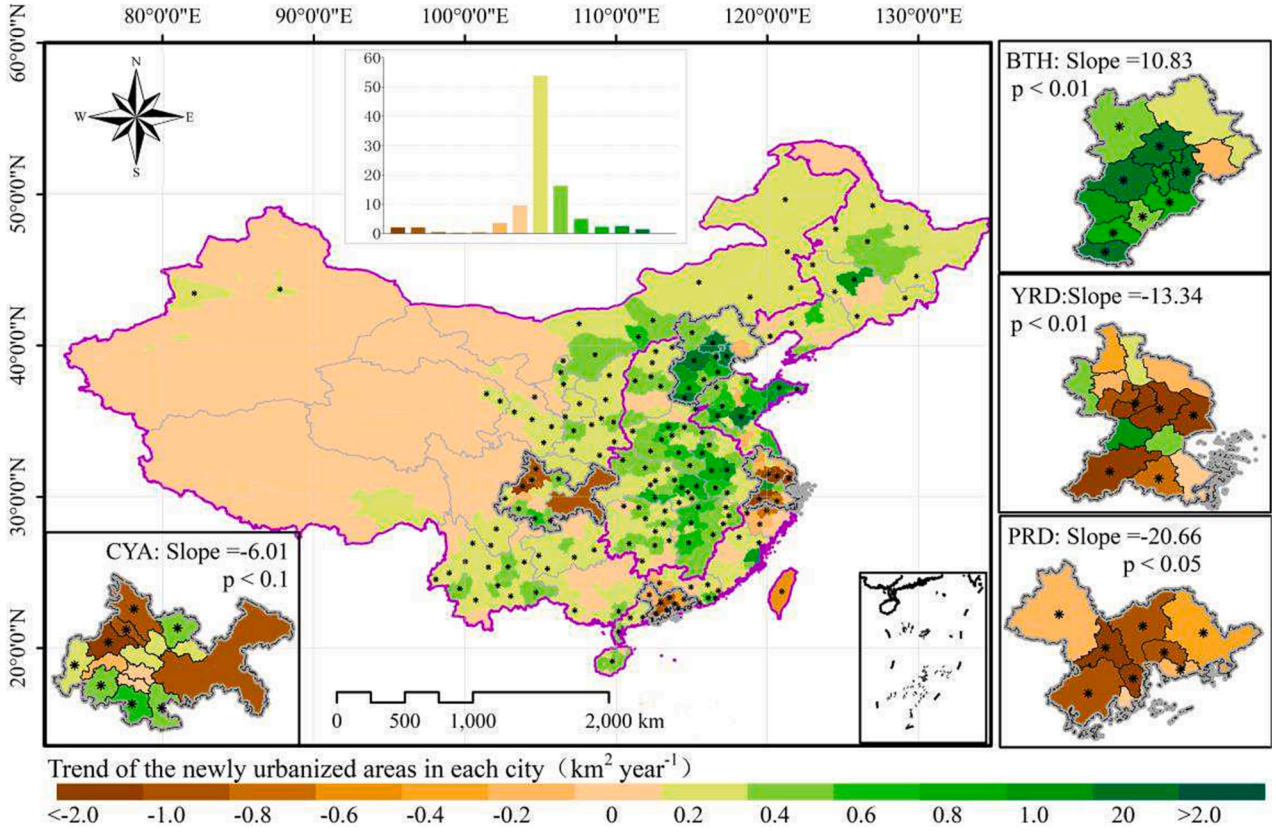

Fig. 3. Spatiotemporal trends of the annual newly urbanized area (i.e., the pixels changed to urban areas in the current year) in China and four urban agglomerations during 2002–2020. Inset shows the percentage of cities with corresponding interannual trends indicated by map legend. BTH, YRD, PRD and CYA denote Beijing-Tianjin-Hebei, Yangtze River Delta, Pearl River Delta and Cheng-Yu Urban Agglomeration, respectively. The symbol of * shows significant trends at $p < 0.05$. The slope is the average rate of change derived from linear regression for the total newly urbanized areas in each urban agglomeration.

entire study period, the average NTL in China significantly increased by 0.48 DN year^{-1} ($p < 0.01$) (Table 2). Notably, the trend of the average NTL in the newly urbanized areas was 0.76 DN year^{-1} ($p < 0.01$), which was higher than the trend in central urban areas (0.46 DN year^{-1}). Similarly, this increasing pattern was found in all regions. Especially, the average NTL in newly urbanized areas in western region increased by 1.37 DN year^{-1} ($p < 0.01$) during this period. The smaller initial value resulted in greater increasing trend. In contrast, the trend of average NTL in urban areas in the northeastern region was smaller than in other regions. In this region, the percentage of areas with decreasing NTL trend in this region was 17.39 % higher than other regions.

Spatially, the average NTL in most cities showed increased trend over the period 2002–2020 (Supplementary Fig. 1). Overall, 288 cities out of 344 (83.72%) showed a significant increasing trend. In contrast, only 3.20% of cities showed significant decreasing trend, which were sparsely located in central and northeastern regions. Generally, the trend of the mean NTL in each city ranged from 0 to 1 DN year^{-1}. The cities with higher trend were mainly located in the southwestern China. This is because these areas have a relatively low economic level in comparison with other areas of China (Yong et al., 2022). With the coordinated regional development policy, the rapid economic growth and rising urbanization quality in this region promoted a rapid growth of the NTL (Yang et al., 2021a).

3.3. Spatiotemporal trend of urban greenness

With the continuous and rapid urban expansion in China, the average EVI_{max} in China significantly decreased by −0.0009 per year ($p < 0.01$) (Fig. 4a). This decreasing trend is more obvious in the newly urbanized areas, with the average EVI_{max} decreased from 0.42 to 0.36 during the period of 2002–2020. The mean trend of average EVI_{max} in the newly urbanized areas was −0.0037 year^{-1}($p < 0.01$) higher than the trend of central urban areas. At regional levels, the average EVI_{max} in the newly urbanized areas in different regions all showed significantly decreasing trends ($p < 0.01$) over this period (Fig. 4b), with the slope of −0.0024, −0.0048, −0.0083 and −0.002 year^{-1}. With this significant decreasing trend, the average EVI_{max} in all urban areas in eastern, central, and western regions decreased significantly ($p < 0.01$). In contrast, the average EVI_{max} in the northeastern region increased significantly ($p < 0.01$), despite a decreasing trend in newly urbanized areas in this region.

Spatially, most cities showed a decrease trend in average EVI_{max}, and 143 cities out of 344 (41.56%) significantly decreased ($p < 0.05$) (Supplementary Fig. 2). In contrast, only 16.28% of cities showing a significant increasing trend, which were mainly located in the northeastern and western regions. Noteworthy, we found an obviously spatial aggregation effect in different mega-urban agglomerations. Specifically, 15.46% of pixels with significant increasing trend ($p < 0.05$) in YRD are usually located in the urban cores. While more pixels (41.28%) in the surrounding of central urban areas showed significantly decreasing trends (Supplementary Fig. 2c). Together with the significant decreasing trends in the annual newly urbanized areas, the average EVI_{max} in YRD deceased by −0.0019 per year ($p < 0.01$). Similar spatial patterns were also found in BTH and CYA, with the significantly decreasing trends of −0.0014 year^{-1}($p < 0.01$) and −0.0023 year^{-1}($p < 0.01$) respectively. In contrast, 36.36% of areas in the central urban region in the PRD showed significant increasing trends, while only 9.97% of pixels decreased significantly. Meanwhile, 23.47% of areas in the newly urbanized region in the PRD also showed significantly increasing trends. Thus, the arerage EVI_{max} in PRD increased by 0.0021 per year ($p < 0.01$).

Table 2
Interannual variability of the average NTL in China different regions during the period of 2002–2020.

	Central urban areas (DN year^{-1})	Newly urbanized areas (DN year^{-1})	All urban areas (DN year^{-1})
Eastern Region	0.42	0.63	0.42
Central Region	0.49	1.00	0.52
Western Region	0.62	1.37	0.68
NorthEastern Region	0.43	0.79	0.46
China	0.46	0.76	0.48

The trends of the NTL are all significant ($p < 0.01$).

3.4. Incoordination relationship between NTL and EVI_{max}

Although the average NTL significantly increased in most cities, the average EVI_{max} significantly decreased in these cities. At the national level, China's decoupling index was less than zero and the relationship of NTL and EVI_{max} was pattern V, indicating a strong incoordination status between urban greenness and economic growth. This strong incoordination status was also found in different regions and agglomerations. Spatially, we found that 64.51% of cities showed a incoordination status, that is, the city had increasing NTL but decreasing EVI_{max} or had decreasing NTL but increasing EVI_{max} (Fig. 5). Notably, 131 cities out of 344 (38.08%) showed significant increasing NTL ($p < 0.05$) but significant decreasing EVI_{max} ($p < 0.05$) (Pattern V), which are mostly located in the eastern, central and western regions. In contrast, 32.55% of cities showed increasing EVI_{max} with the NTL increased during 2002–2020 (DI > 0), which mainly located in the northeastern region and PRD agglomeration.

At pixels levels, only 11.61% of urban areas showed signicantly increasing EVI_{max} and signicantly increasing NTL (Pattern I), while 30.22% of areas showed a strong incoordination status (Pattern V). Similarly, there was a high proportion of areas with the strong incoordination status in the agglomerations of BTH, YRD, and CYA (Fig. 5b–d). In contrast, 63.27% of areas in PRD agglomeration showed a coordination status, and 21.99% of areas showed a strong coordination status (Pattern I).

Moreover, we found that the multi-year average NTL strongly explained the incoordination status between urban greenness and economic growth (Fig. 6). Specifically, in the interval where the multi-year average NTL value is<50, the percetnage of areas with the strong incoordination status (Pattern V)significantly increased by the 1.07% DN $^{-1}$ ($p < 0.01$), but decreased strongly afterward, with the slope of −2.97% DN^{-1} ($p < 0.01$). Based on the annual maximum normalized difference vegetation index ($NDVI_{max}$), this significant threshold effect was also found (Supplementary Fig. 3). Similarly, there is a significant effect in different regions(Fig. 6b, c, d, e). Notably, this threshold of multi-year average NTL value was comparatively larger (TP = 55) in northeastern region (Fig. 6e), which indicated that the urban greenness and economic growth only achieve positive synergies in more developed urban areas.

4. Discussions

4.1. Dramatic uneven urbanization in China

Overall, China had undergone continuous and rapid urban expansion during the 2002–2020, with a mean annual expansion of 1710.96 km^2 year^{-1} ($p < 0.01$) (Fig. 2a). Similarly, this continuous and rapid urban expansion in China was also found by many studies (Liu et al., 2018; Liu et al., 2020). Due to the reform of the urban household registration system and the promotion of compensation rules for land use rights, etc., a considerable number of rural residents swarmed into cities (Chen et al., 2016; Liu et al., 2016; Sun et al., 2020; Liu and Lo, 2022). This rapid urban population growth played a major role in the continuous and rapid urbanization during the period. At regional level, the urban expansion rate of the eastern region was obvious higher than ohter regions. It may be attributed to the differences in socioeconomic and political conditions between different regions (Lu et al., 2019; Liu and Lo, 2022). Specifically, as the most developed region of China, eastern region with urban areas comprised of 51.69% of the total urban area in

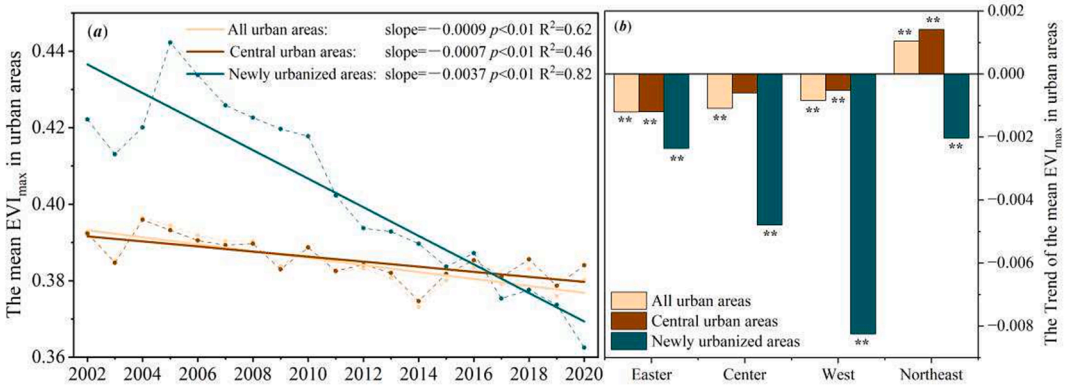

Fig. 4. Interannual variability of the average EVI_{max} in different urban areas (a) and regions (b) in China during the period of 2002–2020. The slope is the average rate of change. The symbol ** indicates the significant trend ($p < 0.01$).

China in 2020 has a higher population growth and the pursuit of economic and was much bettern developed (Ning et al., 2022). Notably, more quota of newly urbanized areas was transferring from eastern region to the central and northeastern region, despite of the highest increasing trend in eastern region. That is, although the urban area in different regions all increased continuously, the urban expansion in the eastern region was slowing, while the expansion rates in the central, western, and northeastern region were growing (Fig. 2b). In particular, this decreasing trend was more obvious in YRD and PRD agglomerations in the eastern region. This transfer of newly urbanized areas was mainly attributed to the considerable efforts and coordinated regional development policies, for example, the Western Development Program, the Revitalize Northeast China Program and the Rise of Central China Plan (Jia et al., 2020). In contrast, the land quotas for urban development were mainly limited by central government in these aggregations (Liu et al., 2014; Fang and Tian, 2020).

4.2. Tough challenge for achieving positive synergies between urban greenness and economic growth

Economic growth was regarded as a major driver for the improvement of urban vegetation (He et al., 2020; Qiao and Huang, 2022). Based on a harmonized nighttime light dataset, the average NTL in China significantly increased during this rapid and dramatic urbanization period. Spatially, the average NTL in most cities (83.72%) showed signifiant increasing trend. This is because the rapid demographic changes and economic activities resulted in the urban night sky has become brighter and brighter in recent decades (Shi et al., 2016b; Liu et al., 2022). However, the average EVI_{max} in most cities decreased significantly. At the national level, urban greenness and economic growth showed a strong incoordination status, which indicates the tough challenge for achieving positive synergies. Spatially, 64.51% of cities showed a incoordination status, and 131 cities out of 344 (38.08%) showed significant increasing NTL ($p < 0.05$) but significant decreasing EVI_{max} ($p < 0.05$) (Strong incoordination status, V), which are mostly located in the eastern, central and western regions. Generally, sustainable economic development did not further improve urban greenness at the national and city scale.

In contrast, some cities with coordination status were only found in northeastern region and PRD agglomeration. However, the percentage of cities with stong corrdination status (Pattern I) was only 11.73%. In the northeastern region, this coordination status was likely caused by the climate in urban areas. Because of the vegetation growth was more sensitive to the urban heat in this in cold areas (Li et al., 2019; Wohlfahrt et al., 2019; Wang et al., 2022). The global warming was enhancing vegetation growth (Zhu et al., 2016; Piao et al., 2020), while some severe urban shrinkage occurred in this region (Yang and Pan, 2020; Yang et al., 2021b). In contrast, in this leading region in China in terms of economic development and ecological protection, this coordination status mainly caused by the stringent and effective measures to build the urban green development zone in the PRD region(Wang et al., 2018; Hu and Xia, 2019; Liang et al., 2021), which demonstrated the considerable efforts for achieving positive synergies.

4.3. Thresholds of incoordination status

At pixels levels, 11.61% of urban areas showed signicant increasing EVI_{max} and signicant increasing NTL (Pattern I), which are mainly found in urban cores. This greening result was also found in many previous studies (Wang et al., 2019; Li et al., 2020a; Qiu et al., 2020; Sun et al., 2020; Chen et al., 2022b). Generally, this positive synergies was attributed by the many resources invested in the construction of infrastructure with the rapid economic growth (Lu et al., 2019; Jia et al., 2020). In these urban cores, with the rapid economic growth, government played more attention and management to improve ecological environment, any newly added street vegetation and green spaces will improve the urban greenness (Li et al., 2018; Li et al., 2020a; Sun et al., 2020; Wang et al., 2022). In contrast, 30.22% of areas showed a strong incoordination status (Pattern V), which are mainly located in the urban surrouding areas. This strong incoordination status was mainly caused by a high demand of land and energy accompanied by rapid economic growth(Jin et al., 2008; Li et al., 2020a; Liu et al., 2020).

Generally, the rapid economic growth resulted in the greening and browning of vegetation in the different urban areas. According to this spatial differentiation pattern of, a threshold effect may be present to explain whether economic growth and urban greenness can achieve positive synergies. That is, this threshold demonstrates when the strong incoordination status will be mitigated significantly. Actually, the multi-year average NTL strongly explained this spatial differentiation of the strong incoordination status. In the areas with the multi-year average NTL value<50, this strong incoordination status was significantly increased, but decreased strongly afterwards with economic growth. In these regions with a high multi-year average NTL value, that is, high economic environment, economic growth encouraged the demand for high quality living environments, particularly an increase urban green space (Richards et al., 2017; He et al., 2020; Li et al., 2020a). While the ecosystem degradation caused by economic growth is still a significant depletion of sustainable urban development before the economic conditions reach this threshold.

4.4. Uncertainties and further studies

Based on the MODIS land cover type product, urban areas were extracted in our study. However, the urban features may be distorted when using this coarsening products (Li et al., 2022). Hence, the different spatio-temporal relationships between the vegetation dynamic

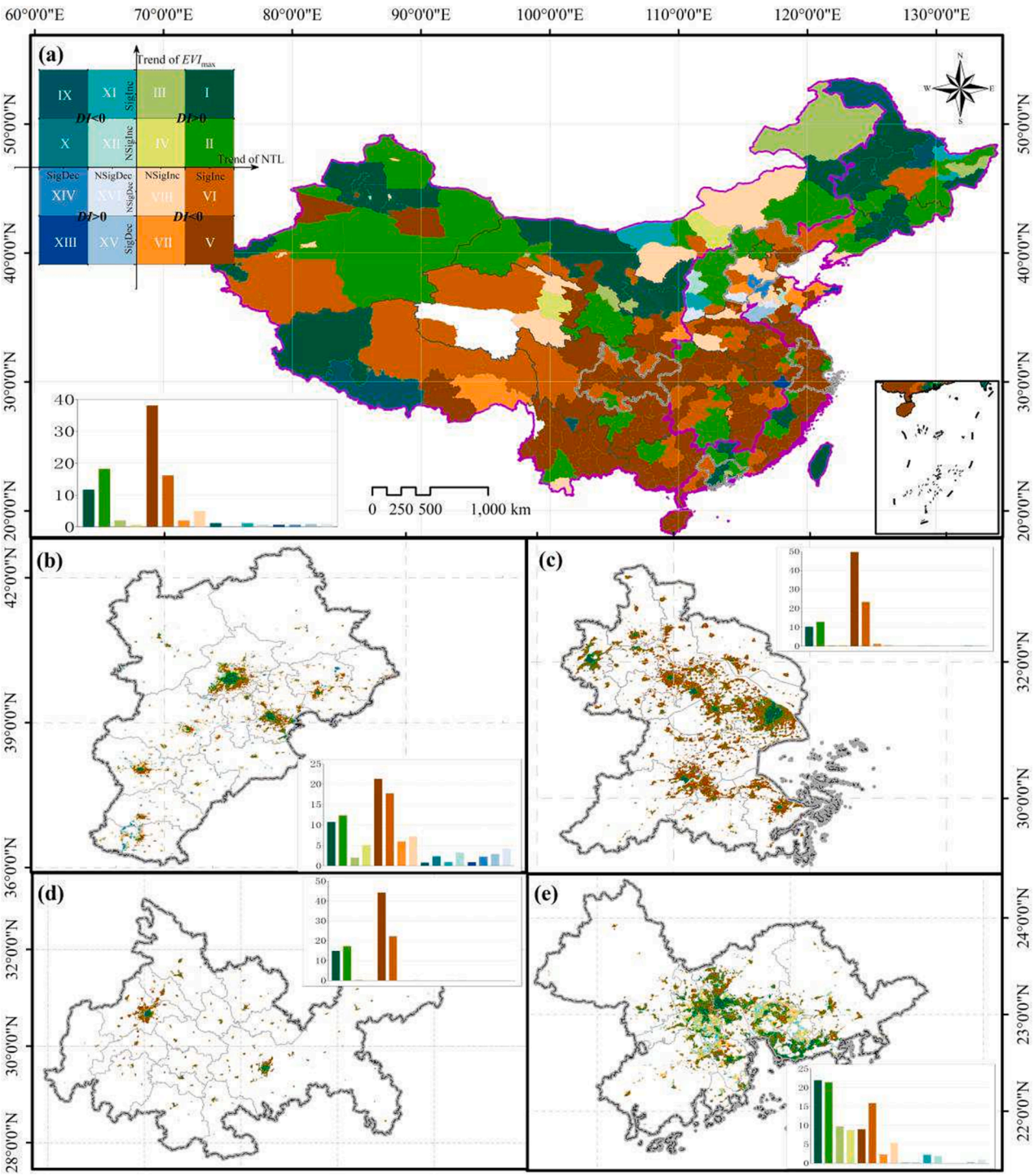

Fig. 5. The spatial distribution of the different relationships of the average EVI_{max} and NTL in all urban areas in China (a) and four agglomerations (b, Beijing-Tianjin-Hebei region. c, Yangtze River Delta. d, Pearl River Delta. e, Cheng-Yu Urban agglomeration). The top inset in (a) indicates the different relationships. DI indicates the decoupling index. Bottom inset in (a) shows the percentage of cities of corresponding relationship indicated by the top inset in (a). Insets in (b, c, d, and e) show the percentage of urban areas of corresponding relationship indicated by the top inset in (a).

and economic growth needs to be further explored based on the higher quality land use data with higher spatial resolution. In addition, there is considerable uncertainty regarding the NTL (Wang et al., 2021; Zheng et al., 2022). Although, we used an integrated and consistent NTL dataset to characterize the urban economic growth, it is impossible to eliminate all noise caused by varying lighting sources (Li et al., 2020b). As a result, it is necessary to further mitigate these uncertainties by using more models and more indicators like housing prices, road connectivity, land use diversity, and POI density, etc. to explore the different relationships of urban greenness and economic growth.

5. Conclusions

In this study, we identified the characteristics of urbanization for each city in different regions and four typical mega-urban agglomerations in China in terms of remote sensing land cover type product, and

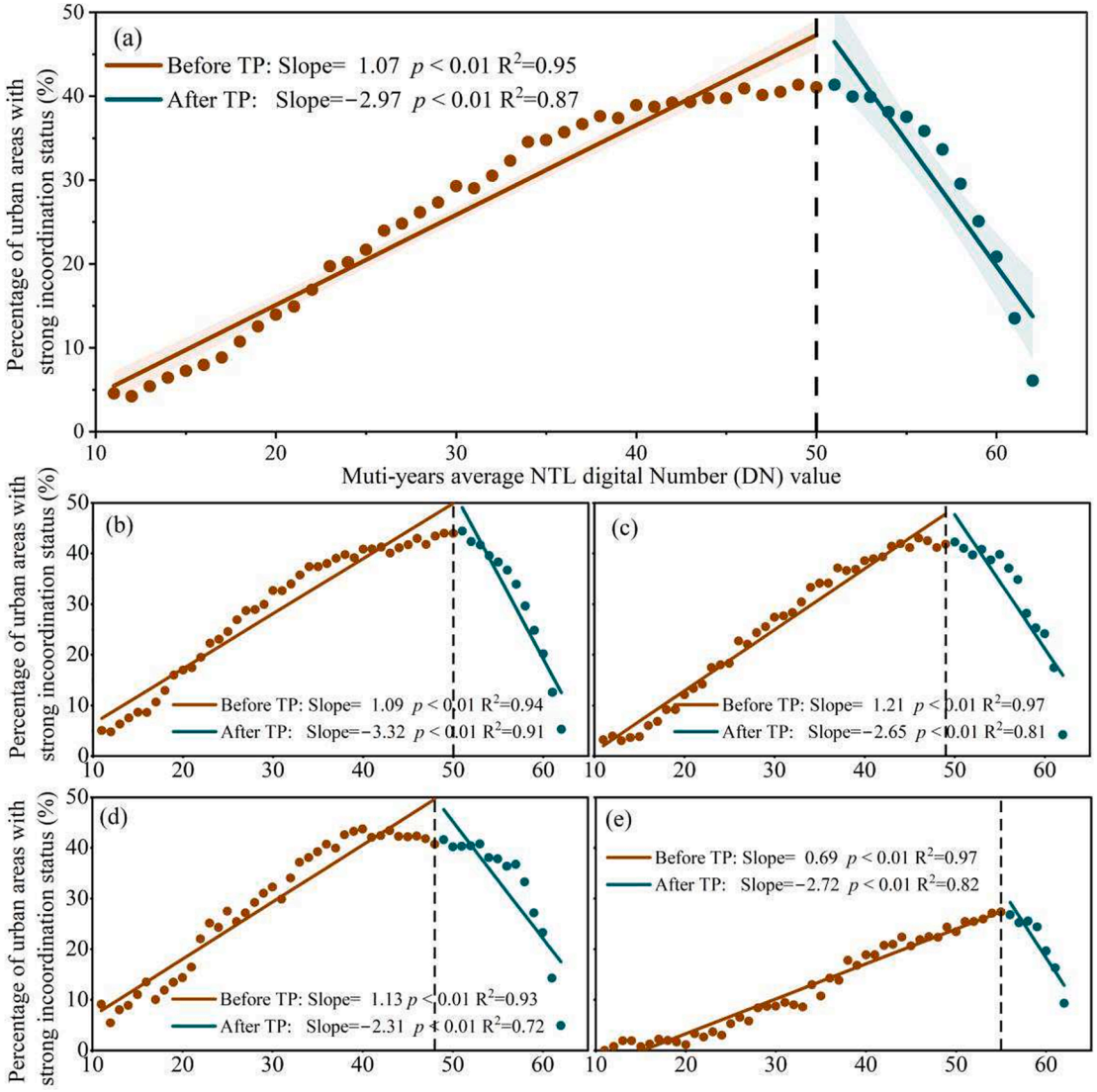

Fig. 6. The relationship between the proportion of areas with a strong incoordination status (Pattern V) and the long-term average NTL in China (a) and Eastern (b), Central (c), Western (d), and Northeastern (e) regions. Solid and dashed line represents linear regression. The dash line in each figure indicates TP. The potential turning point was detected from the piecewise linear regression. The shaded area represents the 95% confidence interval, and the slope is the average rate of change derived from linear regression before and after the turning point, respectively. *p* value denotes significance.

analysed the spatiotemporal characteristics of the EVI_{max} and NTL. Based on their different trends, the different relationships between vegetation dynamic and economic growth were explored during the rapid urbanization period. Generally, China had undergone continuous and rapid urban expansion during the 2002–2020. Notably, more quota of newly urbanized areas was transferring from eastern region to the central and northeastern region. In particular, this significant decreasing trend in annual newly urbanized areas was obvious in the YRD and PRD because of the limit of annual land quotas under the context of coordinated regional development policies. As an original conceive for urban sustainability, economic development will improve urban greening Unfortunately, we found that the mean NTL in most cities increased significantly, while the mean EVI_{max} showed a significant decreasing trend during the continuous and rapid urban expansion period. Spatially, >60% of cities showed a incoordination status. At pixels levels, only 11.61% of urban areas showed signicantly increasing EVI_{max} and signicantly increasing NTL, while 30.22% of areas showed a strong incoordination status. Overall, these spatial heterogeneities of incoordination status in China showed a significant threshold effect. Urban greening and economic growth are coordinated by their different spatial distribution characteristics and relationships. Our study identified a quantitative threshold to explain these different spatial distribution characteristics and relationships, which will be a critical indicator for decision-makers in analysing the different levels of ecological civilization construction in different regions.

Funding

This work was supported by National Natural Science Foundation of China (No. 41901062 and No. 42271310), the Natural Science Foundation of Zhejiang Province (No. LY22D010009).

CRediT authorship contribution statement

Min Cheng: Conceptualization, Methodology, Writing – original draft. **Shaohua Wu:** Conceptualization, Supervision, Writing – review & editing. **Canying Zeng:** Visualization, Writing – review & editing. **Xiaolu Yu:** Data curation, Software. **Jingyi Wang:** Data curation, Software.

Declaration of Competing Interest

The authors declare that they have no known competing financial interests or personal relationships that could have appeared to influence the work reported in this paper.

Data availability

Data will be made available on request.

Appendix A. Supplementary data

Supplementary data to this article can be found online at https://doi.org/10.1016/j.ecolind.2023.110250.

References

Chen, X., Nordhaus, W.D., 2011. Using luminosity data as a proxy for economic statistics. Proceedings of the National Academy of Sciences 108, 8589-8594. 10.1073/pnas.1017031108.

Chen, J., Gao, M., Cheng, S., Hou, W., Song, M., Liu, X., Liu, Y., 2022a. Global 1 km × 1 km gridded revised real gross domestic product and electricity consumption during 1992–2019 based on calibrated nighttime light data. Sci. Data 9, 202. https://doi.org/10.1038/s41597-022-01322-5.

Chen, Y., Ge, Y., Yang, G., Wu, Z., Du, Y., Mao, F., Liu, S., Xu, R., Qu, Z., Xu, B., Chang, J., 2022b. Inequalities of urban green space area and ecosystem services along urban center-edge gradients. Landsc. Urban Plan. 217, 104266 https://doi.org/10.1016/j.landurbplan.2021.104266.

Chen, M., Liu, W., Lu, D., 2016. Challenges and the way forward in China's new-type urbanization. Land Use Pol. 55, 334–339. https://doi.org/10.1016/j.landusepol.2015.07.025.

Cheng, M., Wang, Y., Zhu, J., Pan, Y., 2022. Precipitation dominates the relative contributions of climate factors to grasslands spring phenology on the tibetan plateau. Remote Sens. 14 https://doi.org/10.3390/rs14030517.

Cui, Y., Xiao, X., Dong, J., Zhang, Y., Qin, Y., Doughty, R.B., Wu, X., Liu, X., Joiner, J., Moore, B., 2022. Continued Increases of Gross Primary Production in Urban Areas during 2000-;2016. J. Remote Sensing 2022. https://doi.org/10.34133/2022/9868564.

Didan, K. 2021.MODIS/Terra Vegetation Indices 16-Day L3 Global 500m SIN Grid V061. NASA EOSDIS Land Processes DAAC. Accssed online: https://doi.org/10.5067/MODIS/MOD13A1.061. Accessed on 2022-09-21.

Dobbs, C., Nitschke, C., Kendal, D., 2017. Assessing the drivers shaping global patterns of urban vegetation landscape structure. Sci. Total Environ. 592, 171–177. https://doi.org/10.1016/j.scitotenv.2017.03.058.

Fang, L., Tian, C., 2020. Construction land quotas as a tool for managing urban expansion. Landsc. Urban Plan. 195, 103727 https://doi.org/10.1016/j.landurbplan.2019.103727.

Feng, R., Wang, K., 2022. The direct and lag effects of administrative division adjustment on urban expansion patterns in Chinese mega-urban agglomerations. Land Use Pol. 112, 105805 https://doi.org/10.1016/j.landusepol.2021.105805.

Friedl, M., Sulla-Menashe, D., 2019. MODIS/Terra+Aqua Land Cover Type Yearly L3 Global 500m SIN Grid V006.NASA EOSDIS Land Processes DAAC. Accssed online. https://doi.org/10.5067/MODIS/MCD12Q1.006. Accessed on 2022-03-24.

Fu, B., Wang, S., Zhang, J., Hou, Z., Li, J., 2019. Unravelling the complexity in achieving the 17 sustainable-development goals. Natl. Sci. Rev. 6, 386–388. https://doi.org/10.1093/nsr/nwz038.

Fu, B., Zhang, J., Wang, S., Zhao, W., 2020. Classification–coordination–collaboration: a systems approach for advancing Sustainable Development Goals. Natl. Sci. Rev. 7, 838–840. https://doi.org/10.1093/nsr/nwaa048.

He, Z., Xiao, L., Guo, Q., Liu, Y., Mao, Q., Kareiva, P., 2020. Evidence of causality between economic growth and vegetation dynamics and implications for sustainability policy in Chinese cities. J. Clean Prod. 251, 119550 https://doi.org/10.1016/j.jclepro.2019.119550.

Hou, X., Wu, S., Chen, D., Cheng, M., Yu, X., Yan, D., Dang, Y., Peng, M., 2021. Can urban public services and ecosystem services achieve positive synergies? Ecol. Indic. 124, 107433 https://doi.org/10.1016/j.ecolind.2021.107433.

Hu, M., Xia, B., 2019. A significant increase in the normalized difference vegetation index during the rapid economic development in the Pearl River Delta of China. Land Degradation & Development 30, 359–370. https://doi.org/10.1002/ldr.3221.

Jia, M., Liu, Y., Lieske, S.N., Chen, T., 2020. Public policy change and its impact on urban expansion: an evaluation of 265 cities in China. Land Use Pol. 97, 104754 https://doi.org/10.1016/j.landusepol.2020.104754.

Jin, X.M., Wan, L., Zhang, Y.K., Schaepman, M., 2008. Impact of economic growth on vegetation health in China based on GIMMS NDVI. Int. J. Remote Sens. 29, 3715–3726. https://doi.org/10.1080/01431160701772542.

Levin, N., Kyba, C.C.M., Zhang, Q., Sánchez de Miguel, A., Román, M.O., Li, X., Portnov, B.A., Molthan, A.L., Jechow, A., Miller, S.D., Wang, Z., Shrestha, R.M., Elvidge, C.D., 2020. Remote sensing of night lights: a review and an outlook for the future. Remote Sens. Environ. 237, 111443 https://doi.org/10.1016/j.rse.2019.111443.

Li, X., Chen, G., Zhang, Y., Yu, L., Du, Z., Hu, G., Liu, X., 2022. The impacts of spatial resolutions on global urban-related change analyses and modeling. iScience 25, 105660. https://doi.org/10.1016/j.isci.2022.105660.

Li, D., Stucky, B.J., Deck, J., Baiser, B., Guralnick, R.P., 2019. The effect of urbanization on plant phenology depends on regional temperature. Nat. Ecol. Evol. 3, 1661–1667. https://doi.org/10.1038/s41559-019-1004-1.

Li, F., Wang, X., Liu, H., Li, X., Zhang, X., Sun, Y., Wang, Y., 2018. Does economic development improve urban greening? Evidence from 289 cities in China using spatial regression models. Environ. Monit. Assess. 190, 541. https://doi.org/10.1007/s10661-018-6871-4.

Li, D., Wu, S., Liang, Z., Li, S., 2020a. The impacts of urbanization and climate change on urban vegetation dynamics in China. Urban For. Urban Green. 54, 126764 https://doi.org/10.1016/j.ufug.2020.126764.

Li, L., Zhan, W., Ju, W., Peñuelas, J., Zhu, Z., Peng, S., Zhu, X., Liu, Z., Zhou, Y., Li, J., Lai, J., Huang, F., Yin, G., Fu, Y., Li, M., Yu, C., 2023. Competition between biogeochemical drivers and land-cover changes determines urban greening or browning. Remote Sens. Environ. 287, 113481 https://doi.org/10.1016/j.rse.2023.113481.

Li, X., Zhou, Y., Zhao, M., Zhao, X., 2020b. A harmonized global nighttime light dataset 1992–2018. Sci. Data 7, 168. https://doi.org/10.1038/s41597-020-0510-y.

Liang, L.-N., Siu, W.S., Wang, M.-X., Zhou, G.-J., 2021. Measuring gross ecosystem product of nine cities within the Pearl River Delta of China. Environ. Challenges 4, 100105. https://doi.org/10.1016/j.envc.2021.100105.

Lin, J., Wu, W., 2019. Investigating the land use characteristics of urban integration based on remote sensing data: experience from Guangzhou and Foshan. Geocarto International 34, 1608–1620. https://doi.org/10.1080/10106049.2018.1506505.

Liu, Y., Fang, F., Li, Y., 2014. Key issues of land use in China and implications for policy making. Land Use Pol. 40, 6–12. https://doi.org/10.1016/j.landusepol.2013.03.013.

Liu, X., Hu, G., Chen, Y., Li, X., Xu, X., Li, S., Pei, F., Wang, S., 2018. High-resolution multi-temporal mapping of global urban land using Landsat images based on the Google Earth Engine Platform. Remote Sens. Environ. 209, 227–239. https://doi.org/10.1016/j.rse.2018.02.055.

Liu, X., Huang, Y., Xu, X., Li, X., Li, X., Ciais, P., Lin, P., Gong, K., Ziegler, A.D., Chen, A., Gong, P., Chen, J., Hu, G., Chen, Y., Wang, S., Wu, Q., Huang, K., Estes, L., Zeng, Z., 2020. High-spatiotemporal-resolution mapping of global urban change from 1985 to 2015. Nat. Sustain. 3, 564–570. https://doi.org/10.1038/s41893-020-0521-x.

Liu, M., Liu, X., Zhang, B., Li, Y., Luo, T., Liu, Q., 2022. Analysis of the evolution of urban nighttime light environment based on time series. Sustain. Cit. Soc. 78, 103660 https://doi.org/10.1016/j.scs.2021.103660.

Liu, M., Lo, K., 2022. The territorial politics of urban expansion: Administrative annexation and land acquisition. Cities 126, 103704. https://doi.org/10.1016/j.cities.2022.103704.

Liu, X., Pei, F., Wen, Y., Li, X., Wang, S., Wu, C., Cai, Y., Wu, J., Chen, J., Feng, K., Liu, J., Hubacek, K., Davis, S.J., Yuan, W., Yu, L., Liu, Z., 2019. Global urban expansion offsets climate-driven increases in terrestrial net primary productivity. Nat. Commun. 10, 5558. https://doi.org/10.1038/s41467-019-13462-1.

Liu, F., Zhang, Z., Shi, L., Zhao, X., Xu, J., Yi, L., Liu, B., Wen, Q., Hu, S., Wang, X., Zuo, L., Li, N., Li, M., 2016. Urban expansion in China and its spatial-temporal differences over the past four decades. J. Geogr. Sci. 26, 1477–1496. https://doi.org/10.1007/s11442-016-1339-3.

Lu, Y., Zhang, Y., Cao, X., Wang, C., Wang, Y., Zhang, M., Ferrier, R.C., Jenkins, A., Yuan, J., Bailey, M.J., Chen, D., Tian, H., Li, H., von Weizsäcker, E.U., Zhang, Z., 2019. Forty years of reform and opening up: China's progress toward a sustainable path. Sci. Adv. 5, eaau9413. https://doi.org/10.1126/sciadv.aau9413.

McCallum, I., Kyba, C.C.M., Bayas, J.C.L., Moltchanova, E., Cooper, M., Cuaresma, J.C., Pachauri, S., See, L., Danylo, O., Moorthy, I., Lesiv, M., Baugh, K., Elvidge, C.D., Hofer, M., Fritz, S., 2022. Estimating global economic well-being with unlit settlements. Nat. Commun. 13, 2459. https://doi.org/10.1038/s41467-022-30099-9.

Ning, Y., Liu, S., Zhao, S., Liu, M., Gao, H., Gong, P., 2022. Urban growth rates, trajectories, and multi-dimensional disparities in China. Cities 126, 103717. https://doi.org/10.1016/j.cities.2022.103717.

Normile, D., 2016. China rethinks cities. Science 352, 916–918. https://doi.org/10.1126/science.352.6288.916.

Peng, J., Tian, L., Liu, Y., Zhao, M., Hu, Y.N., Wu, J., 2017. Ecosystem services response to urbanization in metropolitan areas: thresholds identification. Sci. Total Environ. 607–608, 706–714. https://doi.org/10.1016/j.scitotenv.2017.06.218.

Piao, S., Wang, X., Park, T., Chen, C., Lian, X., He, Y., Bjerke, J.W., Chen, A., Ciais, P., Tømmervik, H., Nemani, R.R., Myneni, R.B., 2020. Characteristics, drivers and feedbacks of global greening. Nat. Rev. Earth Environ. 1, 14–27. https://doi.org/10.1038/s43017-019-0001-x.

Qiao, W., Huang, X., 2022. The impact of land urbanization on ecosystem health in the Yangtze River Delta urban agglomerations, China. Cities 130, 103981. https://doi.org/10.1016/j.cities.2022.103981.

Qiu, T., Song, C., Zhang, Y., Liu, H., Vose, J.M., 2020. Urbanization and climate change jointly shift land surface phenology in the northern mid-latitude large cities. Remote Sens. Environ. 236, 111477 https://doi.org/10.1016/j.rse.2019.111477.

R Core Team, 2021. R: A Language and Environment for Statistical Computing. R Foundation for Statistical Computing, Vienna, Austria.

Richards, D.R., Passy, P., Oh, R.R.Y., 2017. Impacts of population density and wealth on the quantity and structure of urban green space in tropical Southeast Asia. Landsc. Urban Plan. 157, 553–560. https://doi.org/10.1016/j.landurbplan.2016.09.005.

Ruan, Y., Zhang, X., Xin, Q., Ao, Z., Sun, Y., 2019. Enhanced vegetation growth in the urban environment across 32 cities in the northern hemisphere. J. Geophys. Res.-Biogeosci. 124, 3831–3846. https://doi.org/10.1029/2019JG005262.

Shahtahmassebi, A.R., Li, C., Fan, Y., Wu, Y., Lin, Y., Gan, M., Wang, K., Malik, A., Blackburn, G.A., 2021. Remote sensing of urban green spaces: a review. Urban For. Urban Green. 57, 126946 https://doi.org/10.1016/j.ufug.2020.126946.

Shan, Y., Fang, S., Cai, B., Zhou, Y., Li, D., Feng, K., Hubacek, K., 2021. Chinese cities exhibit varying degrees of decoupling of economic growth and CO2 emissions between 2005 and 2015. One Earth 4, 124–134. https://doi.org/10.1016/j.oneear.2020.12.004.

Shi, K., Yu, B., Huang, Y., Hu, Y., Yin, B., Chen, Z., Chen, L., Wu, J., 2014. Evaluating the ability of NPP-VIIRS nighttime light data to estimate the gross domestic product and the electric power consumption of china at multiple scales: a comparison with DMSP-OLS Data. Remote Sens. 6, 1705–1724. https://doi.org/10.3390/rs6021705.

Shi, K., Chen, Y., Yu, B., Xu, T., Chen, Z., Liu, R., Li, L., Wu, J., 2016a. Modeling spatiotemporal CO2 (carbon dioxide) emission dynamics in China from DMSP-OLS nighttime stable light data using panel data analysis. Appl. Energy 168, 523–533. https://doi.org/10.1016/j.apenergy.2015.11.055.

Shi, K., Chen, Y., Yu, B., Xu, T., Yang, C., Li, L., Huang, C., Chen, Z., Liu, R., Wu, J., 2016b. Detecting spatiotemporal dynamics of global electric power consumption using DMSP-OLS nighttime stable light data. Appl. Energy 184, 450–463. https://doi.org/10.1016/j.apenergy.2016.10.032.

Sulla-Menashe, D., Gray, J.M., Abercrombie, S.P., Friedl, M.A., 2019. Hierarchical mapping of annual global land cover 2001 to present: the MODIS Collection 6 Land Cover product. Remote Sens. Environ. 222, 183–194. https://doi.org/10.1016/j.rse.2018.12.013.

Sun, L., Chen, J., Li, Q., Huang, D., 2020. Dramatic uneven urbanization of large cities throughout the world in recent decades. Nat. Commun. 11, 5366. https://doi.org/10.1038/s41467-020-19158-1.

Wang, L., De Boeck, H.J., Chen, L., Song, C., Chen, Z., McNulty, S., Zhang, Z., 2022. Urban warming increases the temperature sensitivity of spring vegetation phenology at 292 cities across China. Sci. Total Environ. 834, 155154 https://doi.org/10.1016/j.scitotenv.2022.155154.

Wang, S., Ju, W., Peñuelas, J., Cescatti, A., Zhou, Y., Fu, Y., Huete, A., Liu, M., Zhang, Y., 2019. Urban−rural gradients reveal joint control of elevated CO2 and temperature on extended photosynthetic seasons. Nat. Ecol. Evol. 3, 1076–1085. https://doi.org/10.1038/s41559-019-0931-1.

Wang, Z., Román, M.O., Kalb, V.L., Miller, S.D., Zhang, J., Shrestha, R.M., 2021. Quantifying uncertainties in nighttime light retrievals from Suomi-NPP and NOAA-20 VIIRS Day/Night Band data. Remote Sens. Environ. 263, 112557 https://doi.org/10.1016/j.rse.2021.112557.

Wang, M.-X., Zhao, H.-H., Cui, J.-X., Fan, D., Lv, B., Wang, G., Li, Z.-H., Zhou, G.-J., 2018. Evaluating green development level of nine cities within the Pearl River Delta, China. J. Clean Prod. 174, 315–323. https://doi.org/10.1016/j.jclepro.2017.10.328.

Wohlfahrt, G., Tomelleri, E., Hammerle, A., 2019. The urban imprint on plant phenology. Nat. Ecol. Evol. 3, 1668–1674. https://doi.org/10.1038/s41559-019-1017-9.

Wu, Y., Zhang, X., Shen, L., 2011. The impact of urbanization policy on land use change: a scenario analysis. Cities 28, 147–159. https://doi.org/10.1016/j.cities.2010.11.002.

Yang, Z., Pan, Y., 2020. Are cities losing their vitality? Exploring human capital in Chinese cities. Habitat Int. 96, 102104 https://doi.org/10.1016/j.habitatint.2019.102104.

Yang, Y., Wu, J., Wang, Y., Huang, Q., He, C., 2021b. Quantifying spatiotemporal patterns of shrinking cities in urbanizing China: A novel approach based on time-series nighttime light data. Cities 118, 103346. https://doi.org/10.1016/j.cities.2021.103346.

Yang, G., Xiao, Y., Da, L., Yu, Z., 2022a. The quantity-quality and gain-loss conversion pattern of green vegetation during urbanization reveals the importance of protecting natural forest ecosystems. Landsc. Ecol. 37, 2929–2945. https://doi.org/10.1007/s10980-022-01519-4.

Yang, W., Yang, R., Zhou, S., 2022b. The spatial heterogeneity of urban green space inequity from a perspective of the vulnerable: a case study of Guangzhou, China. Cities 130, 103855. https://doi.org/10.1016/j.cities.2022.103855.

Yang, L.J., Zhang, X.H., Pan, J.H., Yang, Y.C., 2021a. Coupling coordination and interaction between urbanization and eco-environment in Cheng-Yu urban agglomeration, China. The journal of applied ecology 32, 993–1004. https://doi.org/10.13287/j.1001-9332.202103.012.

Yong, Z., Li, K., Xiong, J., Cheng, W., Wang, Z., Sun, H., Ye, C., 2022. Integrating DMSP-OLS and NPP-VIIRS Nighttime Light Data to Evaluate Poverty in Southwestern China. Remote Sens. 14 https://doi.org/10.3390/rs14030600.

Yuan, W., Zheng, Y., Piao, S., Ciais, P., Lombardozzi, D., Wang, Y., Ryu, Y., Chen, G., Dong, W., Hu, Z., Jain, A.K., Jiang, C., Kato, E., Li, S., Lienert, S., Liu, S., Nabel, J.E. M.S., Qin, Z., Quine, T., Sitch, S., Smith, W.K., Wang, F., Wu, C., Xiao, Z., Yang, S., 2019. Increased atmospheric vapor pressure deficit reduces global vegetation growth. Sci. Adv. 5, eaax1396. https://doi.org/10.1126/sciadv.aax1396.

Zeng, Y., Hao, D., Huete, A., Dechant, B., Berry, J., Chen, J.M., Joiner, J., Frankenberg, C., Bond-Lamberty, B., Ryu, Y., Xiao, J., Asrar, G.R., Chen, M., 2022. Optical vegetation indices for monitoring terrestrial ecosystems globally. Nat. Rev. Earth Environ. 3, 477–493. https://doi.org/10.1038/s43017-022-00298-5.

Zhao, C., Cao, X., Chen, X., Cui, X., 2022. A consistent and corrected nighttime light dataset (CCNL 1992–2013) from DMSP-OLS data. Sci. Data 9, 424. https://doi.org/10.1038/s41597-022-01540-x.

Zhao, J., Chen, S., Jiang, B., Ren, Y., Wang, H., Vause, J., Yu, H., 2013. Temporal trend of green space coverage in China and its relationship with urbanization over the last two decades. Sci. Total Environ. 442, 455–465. https://doi.org/10.1016/j.scitotenv.2012.10.014.

Zheng, Q., Weng, Q., Zhou, Y., Dong, B., 2022. Impact of temporal compositing on nighttime light data and its applications. Remote Sens. Environ. 274, 113016 https://doi.org/10.1016/j.rse.2022.113016.

Zhou, Y., Li, X., Asrar, G.R., Smith, S.J., Imhoff, M., 2018. A global record of annual urban dynamics (1992–2013) from nighttime lights. Remote Sens. Environ. 219, 206–220. https://doi.org/10.1016/j.rse.2018.10.015.

Zhu, Z., Piao, S., Myneni, R.B., Huang, M., Zeng, Z., Canadell, J.G., Ciais, P., Sitch, S., Friedlingstein, P., Arneth, A., Cao, C., Cheng, L., Kato, E., Koven, C., Li, Y., Lian, X., Liu, Y., Liu, R., Mao, J., Pan, Y., Peng, S., Peñuelas, J., Poulter, B., Pugh, T.A.M., Stocker, B.D., Viovy, N., Wang, X., Wang, Y., Xiao, Z., Yang, H., Zaehle, S., Zeng, N., 2016. Greening of the Earth and its drivers. Nature Clim. Change 6, 791–795. https://doi.org/10.1038/nclimate3004.

Zhu, C., Zhang, X., Wang, K., Yuan, S., Yang, L., Skitmore, M., 2020. Urban–rural construction land transition and its coupling relationship with population flow in China's urban agglomeration region. Cities 101, 102701. https://doi.org/10.1016/j.cities.2020.102701.